ORIGINAL ARTICLE

Check for
updates

Analysis of floor-to-column pounding of buildings founded on different soil types

Mahmoud Miari[1] · **Robert Jankowski**[1]

© The Author(s) 2022

Abstract

The aim of this study is to investigate the effect of the soil type on buildings experiencing floor-to-column pounding during earthquakes. Five buildings with 4-storeys, 6-storeys, and 7-storeys were considered. Three types of the 4-storey building with different total heights were taken into account which leads to floor-to-column pounding at 1/3, 1/2 and 2/3 of the height of the impacted column. Two pounding scenarios were considered, i.e. pounding between the 4-storey and 6-storey buildings (three cases when collisions occur at 1/3, 1/2 and 2/3 of the height of the impacted column) and pounding between the 4-storey and 7-storey buildings (three cases when collisions occur at 1/3, 1/2 and 2/3 of the height of the impacted column). In the first part of this study, the shear demands of the columns at the contact area were studied and compared with the no pounding case to investigate the effect of the floor-to-column pounding. Then, the shear demands of the columns at the contact area were studied for buildings founded on different soil types to investigate the effect of the soil type on the structural response. The results of this study illustrate that the shear demands of the impacted column significantly increase due to collisions and it exceeds the shear strength in all cases. Moreover, impacted column experiences higher shear demands for buildings founded on the soft clay soil, then for buildings founded on the stiff soil, then for buildings founded on very dense soil and soft rock, and finally for buildings founded on the rock and hard rock.

Keywords Structural pounding · Floor-to-column impact · Buildings · Soil type · Shear demands · Earthquakes

1 Introduction

Structural interactions between adjacent buildings have been identified as a common cause of damage during seismic excitations. This problem of such collisions between buildings in contact, or with small separation, is known as the earthquake-induced structural pounding. This phenomenon has a significant effect on the response of colliding buildings

✉ Mahmoud Miari
  mahmoud-miari@hotmail.com; mahmoud.miari@pg.edu.pl

1 Department of Construction Management and Earthquake Engineering, Faculty of Civil
   and Environmental Engineering, Gdańsk University of Technology, Gdańsk, Poland

(Anagnostopoulos 1988; Favvata 2017; Kazemi et al. 2021; Mavronicola et al. 2020; Rezaei et al. 2020). It is frequently experienced when strong earthquakes struck big cities and densely populated areas because the buildings in big cities are usually constructed close or in contact with each other due to economic reasons. In certain earthquakes, pounding was identified as the major reason of damage or collapse. This includes the Mexico earthquake where 40% of buildings experienced pounding and in 15% of buildings with severe damage or collapse pounding was found (Rosenblueth and Meli 1986) and where in 20–30% of them pounding was the major reason for damage (Anagnostopoulos 1996). Another example concerns the Loma Prieta earthquake where pounding was found in 200 out of 500 surveyed buildings (Kasai and Maison 1997). Although these earthquakes were somehow unique or overestimated damages due to pounding, pounding was experienced almost in every earthquake, including, for example, the 2010 Darfield earthquake (Cole et al. 2010b, 2011) and in the 2011 Christchurch earthquake (Cole et al. 2012a, b).

The aspects of earthquake-induced pounding have been studied for more than three decades (see, for example, two state-of-the-art papers: Miari et al. 2019, 2021 for details). The main reason that leads to collisions between adjacent structures is the narrow gap commonly provided between them. The seismic gap has been found to have a significant effect on the response of colliding buildings (Jameel et al. 2013; Miari and Jankowski 2022a). Structural pounding leads to the increase in the peak interstorey drift (IDR), residual IDR, floor peak accelerations, shear forces and also it results in the generation of high impact forces while the displacement may increase or decrease (Efraimiadou et al. 2013; Inel et al. 2014; Raheem 2006, 2014; Rojas and Anderson 2012; Sołtysik and Jankowski 2013, 2015). The amplification of the response is experienced in the direction of pounding while the response in the other directions is usually unaffected (Jameel et al. 2013). The degree of amplification depends on the dynamic properties of colliding buildings (natural periods, damping ratios, etc.) (Jankowski 2005, 2006). Moreover, the dilemma between the effect of pounding on stiff and flexible structures is still with no clear results since some studies found that pounding amplified the response of the flexible structure and had an insignificant effect on the stiff structure (Elwardany et al. 2017; Jankowski 2007, 2008; Mahmoud et al. 2008; Mahmoud and Jankowski 2009; Maison and Kasai 1992; Mouzakis and Papadrakakis 2004) while other studies indicated that pounding amplified the response of the stiff structure and suppressed the response of the flexible structure (Gong and Hao 2005; Jankowski et al. 2015). Moreover, the infill panels have a significant influence on the response of buildings experiencing collisions during earthquakes (Elwardany et al. 2019; Karayannis et al. 2005, 2011).

Structural pounding can be classified into two types, i.e. into floor-to-floor pounding and floor-to-column pounding (Cole et al. 2010a). Floor-to-floor pounding is observed when the slab of one building collides with the slab of the other adjacent building. It occurs when the storey heights of both structures are equal. Floor-to-column pounding takes place when the slab of one building collides with the column of the other building. It occurs when the storey heights of both structures are not equal. Specifically, in the case of floor-to-column pounding, the slab of the top storey of the shorter building collides with the columns of the adjacent taller building. Such collisions lead to a significant increase in the ductility demands at and above the contact area and become critical in the case of contact buildings since, in this case, the ductility demand exceeds the available ductility (Karayannis and Favvata 2005a, b). Indeed, such collisions also lead to a significant increase in the shear demands of the columns at and above the contact area and it is critical in all cases where the shear demand exceeds the available shear strength in all cases (Favvata et al. 2009; Karayannis and Favvata 2005a, 2005b).

Also, the shear demands in the case of floor-to-column pounding are critical in the case of torsional pounding where the shear demand also exceeds the available shear strength (Karayannis and Naoum 2017, 2018). Moreover, the floor-to-column pounding has a significant effect in both cases where the collisions occur at the lower/upper part of the column (Doğan and Günaydin 2009) and when pounding takes place at the mid-height of the column (Rajaram and Kumar 2012).

In most of the studies that were focused on earthquake-induced pounding, fixed based buildings were considered. However, the soil-structure interaction (SSI) and the soil-pile-structure interaction may have a significant effect on the response of colliding buildings (Korzec and Jankowski 2021; Fatahi et al. 2018; Naserkhaki et al. 2014; Kamgar et al. 2021). This is due to the fact that the SSI reduces the natural frequency of buildings due to the flexibility induced by the soil/base (Stewart et al. 1999). The flexible structure experiencing pounding and considering SSI is significantly more affected than the stiff one (Ghandil and Aldaikh 2017; Madani et al. 2015; Mahmoud et al. 2013; Naserkhaki et al. 2012). Some studies indicate that the pounding with SSI leads to the increase in the displacements, shear forces and impact forces (see Farghaly 2017; Ghandil and Aldaikh 2017; Kontoni and Farghaly 2018; Li et al. 2017; Naserkhaki et al. 2012, 2013, 2014 for example) while other studies point out that the opposite situation might take place (see Elwardany et al. 2019; Mahmoud et al. 2013; Shakya and Wijeyewickrema 2009; Shakya et al. 2008, for example). These contradictory results are referred for several reasons, including the soil type and foundation type used in different analyses. The SSI effects and the site effects were studied considering and neglecting SSI and it was found that the site effects and SSI had a significant influence on the response of buildings (Behnamfar and Banizadeh 2016; Karapetrou et al. 2015; Requena-Garcia-Cruz et al. 2022). Recently, the effects of the soil type on the response of buildings experiencing collisions during earthquakes have been studied (see Miari and Jankowski 2021, 2022b, c, d, for example). It was found that the soil type has a significant effect on the response of colliding buildings. However, in these studies, only floor-to-floor pounding was considered and floor-to-column pounding was not taken into account.

The literature review illustrates that contradictory results about the effect of SSI on buildings experiencing pounding were obtained in previous studies due to ignoring some factors including the soil type. Indeed, in the very limited studies that considered the effects of the soil type on the response of colliding buildings, floor-to-floor pounding was considered and the floor-to-column pounding was ignored. Therefore, the aim of this study is to investigate the effect of the soil type on buildings experiencing floor-to-column pounding. The shear demands of the column experiencing collisions from the top slab of the adjacent shorter building is of special interest in this study. Five buildings with 4-storeys, 6-storeys, and 7-storeys were considered. Three types of the 4-storey building with different total heights were taken into account which leads to floor-to-column pounding at 1/3, 1/2 and 2/3 of the height of the impacted column. Two pounding scenarios were considered, i.e. pounding between the 4-storey and 6-storey buildings (three cases when collisions occur at 1/3, 1/2 and 2/3 of the height of the impacted column) and pounding between the 4-storey and 7-storey buildings (three cases when collisions occur at 1/3, 1/2 and 2/3 of the height of the impacted column). In the first part of this study, the shear demands of the columns at the contact area were studied and compared with the no pounding case to investigate the effect of the floor-to-column pounding. In the second part, the shear demands of the columns at the contact area were studied for buildings founded on different soil types to investigate the effect of the soil type on the structural response.

2 Numerical models of buildings

Five concrete buildings were considered in this study, i.e. structures with 4-storeys, 6-storeys and 7-storeys. These buildings had a length of 16 m and a width of 20 m (The bays were 4×4 m in the x-direction and 5×4 m in the y-direction). The 6-storey and 7-storey buildings had a 3 m storey height. Three types of the 4-storey building with different storey heights were considered. The first type concerns the 4-storey building with the height of the first storey equal to 4 m and the height of the other storeys equal to 3 m. The second type is the case of the 4-storey building with the height of the first storey equal to 4.5 m and the height of the other storeys equal to 3 m. The third type concerns the 4-storey building with the height of the first and the second storey equal to 4 m and the height of the other storeys equal to 3 m. The first type leads to collisions between the upper slab of the shorter building and the corresponding column of the taller structure at 1/3 h (1/3 of its height), the second type leads to pounding between the upper slab of the shorter building and the corresponding column of the taller building at 1/2 h (1/2 of its height), the third type leads to collisions between the upper slab of the shorter building and the corresponding column of the taller building at 2/3 h (2/3 of its height). The structural models of these buildings were created using ETABS software using the finite element (FE) method. The columns and beams were defined as frame elements and the slabs as shell elements. The FE models of the considered buildings are presented in Fig. 1 in 3-D and elevation views. In this study, the material properties were used as follows: concrete with the compressive strength of 35 MPa and the modulus of elasticity of 27.8 GPa, steel (grade 60) with the yield strength of 420 MPa and the modulus of elasticity of 200 GPa. Indeed, the live load was considered to be equal to 4 kN/m^2, while the superimposed dead load was equal to 2 kN/m^2. The buildings were designed so as to satisfy the minimum reinforcement requirements based on the ACI code (American Concrete Institute). The ACI code 10.9.1 requires the reinforcement ratio to be between 1 and 8% of the concrete area. To ensure the optimum design, as well as the economic design of structural members, the reinforcement ratio in the columns has been taken as equal to 1%.The natural period, frequency and mass for each building are shown in Table 1.

Two pounding scenarios were considered between these buildings, i.e. pounding between the 4-storey and 6-storey buildings (4-6 pounding scenario) and pounding between the 4-storey and 7-storey buildings (4-7 pounding scenario). Since three types of the 4-storey building were used in this study, four cases were defined, i.e. Case 1: when the first type of the 4-storey building is used, Case 2: when the second type of the 4-storey building is used, Case 3: when the third type of the 4-storey building is used and also Case 4 which corresponds to the no pounding case (defined for comparison purposes). The seismic gap was considered as equal to 4 cm for all the cases. In this study, pounding was modelled by the use of special gap elements. These elements are two-node compression-only link elements. They are activated when adjacent buildings are in contact and deactivated elsewhere (see Computers and Structures ETABS reference manual for details). The change from one state into another one makes the model to be nonlinear (geometric nonlinearity). A similar situation concerns support elements implemented in the numerical model of colliding buildings exposed to seismic excitations. Indeed, each nonlinear force–deformation relationship in the gap/support element includes stiffness that has to be determined for each time step (see Computers and Structures ETABS reference manual). If it is considered to be zero in the particular time step, no nonlinear force is generated in the link/support element. In this study, the gap elements were placed every 4 m along the collision length at
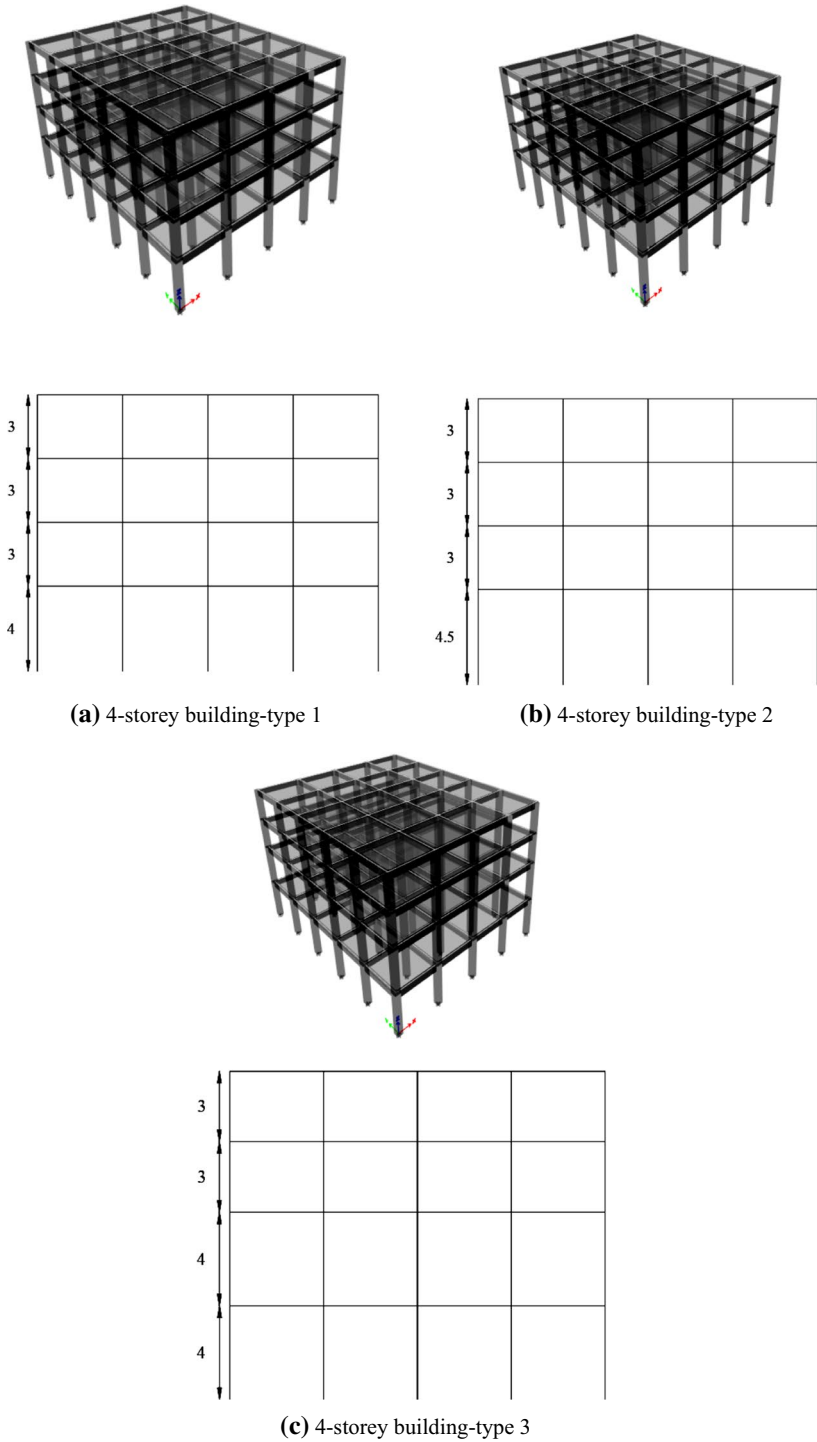
(a) 4-storey building-type 1

(b) 4-storey building-type 2

(c) 4-storey building-type 3

Fig. 1 FE models of the considered buildings in 3-D and elevation views
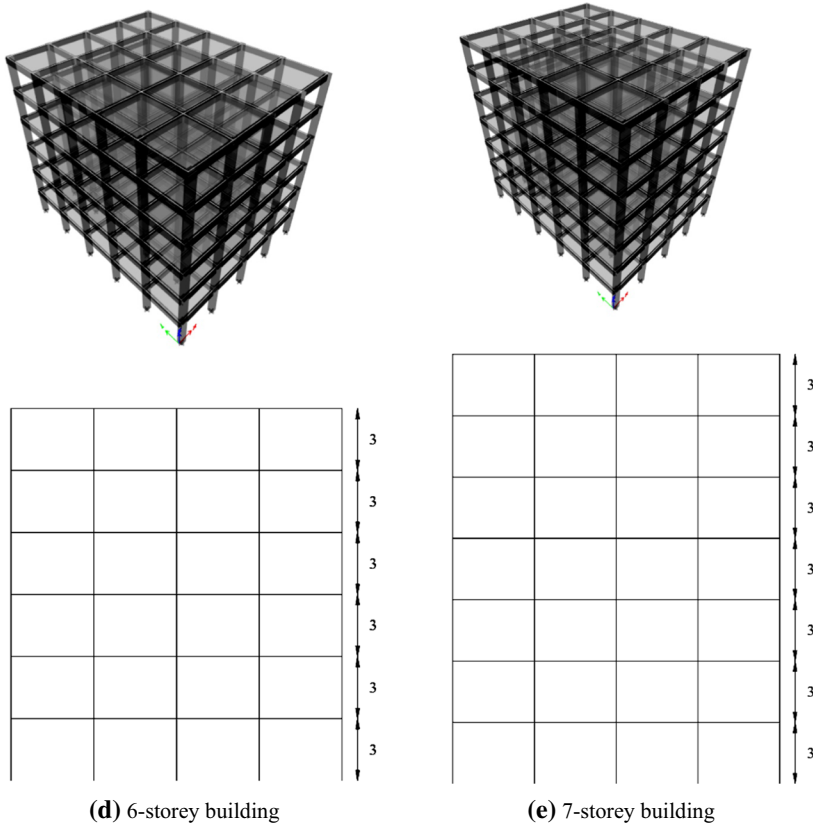
(d) 6-storey building   **(e)** 7-storey building

Fig. 1 (continued)

Table 1 Natural periods, frequencies and masses of buildings

Building	Period (s)	Frequency (Hz)	Mass (ton)
4-storey building Type 1	0.649	1.542	1495.924
4-storey building Type 2	0.71	1.408	1505.483
4-storey building Type 3	0.737	1.357	1515.043
6-storey building	0.829	1.206	2587.084
7-storey building	0.971	1.03	2217.500

all storeys (6 elements at each storey were used). The activation of each gap element is usually implemented in the numerical model with the help of spring having relatively high stiffness (see Ghandil and Aldaikh 2017). This solution allows us to prevent overlapping and results in the deformation of colliding buildings at the points of contact simulating real collision. However, since the geometry of the impact surfaces is unknown, the behaviour of the spring is highly uncertain and therefore the material under the impact loadings present uncertain properties depending on the variable impact velocities. In this study, the spring stiffness was taken as equal to 10^{10} N/m. This value has been found to be large enough so

as to obtain accurate response of buildings experiencing collisions during earthquakes (see Ghandil and Aldaikh 2017). The FE models of the 4-6 and 4-7 pounding scenarios (and the corresponding cases) are presented in Figs. 2 and 3, respectively. The respective ratios of natural periods, frequencies and masses for two buildings in the case of different pounding scenarios are presented in Table 2. It can be seen from the figures that six columns of the taller building (at the 5th storey) were subjected to collisions from the top storey of the 4-storey building in the 4-6 and 4-7 pounding scenarios. These columns are named as C1, C2, C3, C4, C5 and C6 at ordinates 0, 4, 8, 12, 16 and 20 m respectively (see Fig. 4).
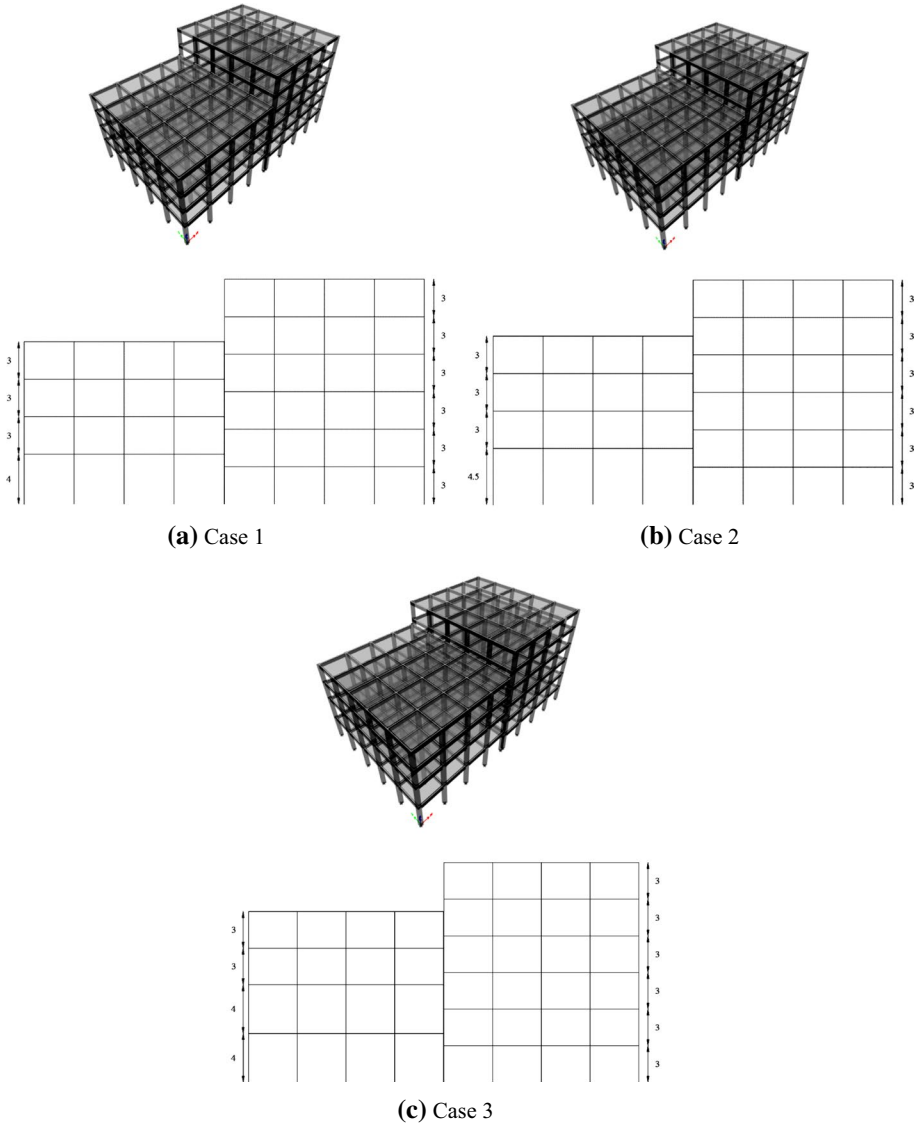

(a) Case 1

(b) Case 2

(c) Case 3

Fig. 2 FE models of the 4-6 pounding scenario in 3-D and elevation views

(a) Case 1

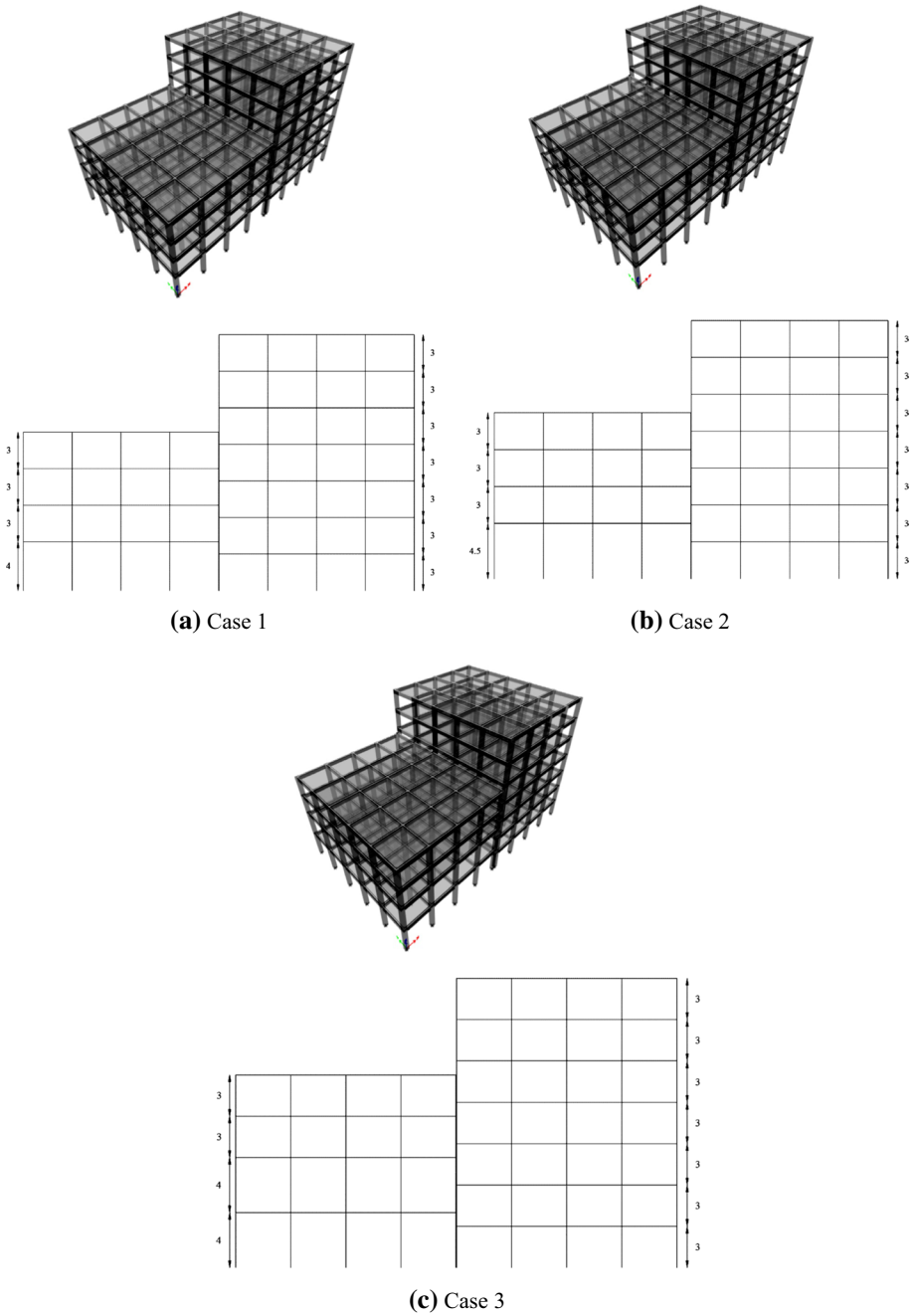**(b)** Case 2

(c) Case 3

Fig. 3 FE models of the 4-7 pounding scenario in 3-D and elevation views

Table 2 Ratios of natural periods, frequencies and masses for two buildings in the case of different pounding scenarios

Pounding scenario	Period ratio (–)	Frequency ratio (–)	Mass ratio (–)
4-6 pounding scenario Case 1	0.783	1.279	0.578
4-6 pounding scenario Case 2	0.856	1.167	0.582
4-6 pounding scenario Case 3	0.889	1.125	0.586
4-7 pounding scenario Case 1	0.668	1.497	0.675
4-7 pounding scenario Case 2	0.731	1.367	0.679
4-7 pounding scenario Case 3	0.759	1.317	0.683

Fig. 4 Plan view of the 6-storey and 7-storey buildings
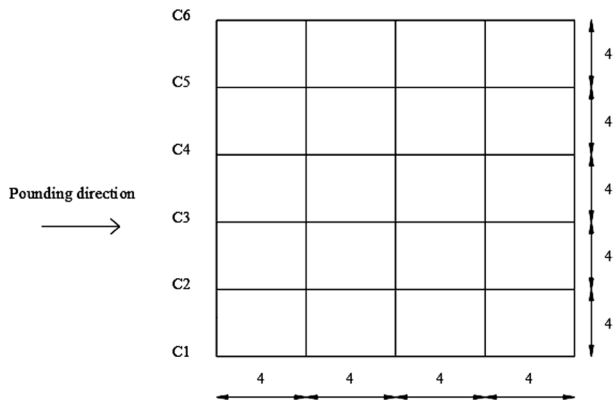
Five soil types defined in the ASCE 7-10 code (American Society of Civil Engineers) were used in this study, i.e. soil type A (hard rock), soil type B (rock), soil type C (very dense soil and soft rock), soil type D (stiff soil) and soil type E (soft clay soil). In this study, the site class/ soil type was considered using the response spectrum concept. The site class was considered by defining the response spectrum corresponding to a specific site class and then by matching the earthquake record with the defined response spectrum. The site properties were defined by three site coefficients: F_a (the short-period site coefficient (at period of 0.2 s)), F_v (the long-period site coefficient (at period of 1 s)) and T_L (the long-period transition period). The first two parameters (F_a and F_v) were defined according to Tables 11.4-1 and 11.4-2 in the ASCE 7-10 code. To evaluate these two parameters, the values of the mapped risk-targeted Maximum Considered Earthquake, MCE_R, spectral response acceleration parameter at short period (S_s) and the mapped risk-targeted MCE_R spectral response acceleration parameter at period of 1 s (S_1) were determined from the 0.2 s and 1 s spectral response accelerations shown in Figures 22-1, 22-3, 22-5, and 22-6 for S_S and Figures 22-2, 22-4, 22-5, and 22-6 for S_1 in the ASCE 7-10 code. The third required parameter for the definition of the response spectrum is T_L shown in Figures 22-12 to 22-16 in the ASCE 7-10 code. It was defined for different regions of the US and the maps include five values of T_L which are 4 s, 6 s, 8 s, 12 s and 16 s. The site parameters were selected as follows: 0.5 for S_1, 1.25 for S_s and additionally 8 s for T_L (Miari and Jankowski 2022b, c). More descriptions about the site class and the selection of the site parameters can be found in the papers: Miari and Jankowski 2022b, 2022c.

The analysis was performed for two earthquake records, i.e. the Kobe earthquake of 1995 (station: Kobe University, peak ground acceleration (PGA) = 0.275766 g) and the Parkfiled earthquake of 1966 (station: San Luis Obispo station, PGA = 0.01175 g)—see PEER website database for details. A time step of 0.001 s was used in this study. The most representative results obtained for the 4-7 pounding scenario under the Parkfield earthquake and the 4-6 pounding scenario under the Kobe earthquake are presented in this study. The structural response was obtained by applying the fast nonlinear analysis method developed by Ibrahimbegovic and Wilson (1989). The nonlinearity was considered for the gap and support elements in this method. The dynamic equilibrium equation of the vibrating structure is shown in Eq. (1).

$$K_L u(t) + C \dot{u}(t) + M \ddot{u}(t) + r_N(t) = -M \ddot{u}_g(t) \tag{1}$$

where K_L is the stiffness matrix for the linear elastic elements (all elements except for the gap and support elements); C is the proportional damping matrix; M is the diagonal mass matrix; $r_N(t)$ is the vector of forces from the nonlinear degrees of freedom (gap and support elements); $u(t)$, $\dot{u}(t)$, and $\ddot{u}(t)$ are vectors of the relative displacements, velocities, and accelerations with respect to the ground; and $\ddot{u}_g(t)$ is the vector of ground motion accelerations (see Ibrahimbegovic and Wilson 1989 for details).

3 Effect of the floor-to-column pounding on the shear demands of the impacted column

In this section, the effect of pounding on the columns of the taller buildings, that experience impact from the slab of the top storey of the shorter building, is investigated. Tables 3 and 4 present the peak shear forces observed in column C4 for the 4-7 and 4-6 pounding scenarios, respectively, for cases 1, 2 and 4. The graphical representation of the results is also shown in Figs. 5 and 6. As it can be seen, the peak shear forces experienced by the impacted columns were significantly increased in the case of pounding (cases 1 and 2) as compared to the no pounding case (case 4). For instance, column C4 founded on soil type A has experienced shear force of 449.7 kN in case 1, 449.1 kN in case 2 and 256.1 kN in case 4 for the 4-7 pounding scenario. The ratio between the peak shear forces experienced by the impacted column (C4) in the case of pounding to that of the no pounding case has been calculated also in Tables 3 and 4. This ratio was found to be between 2 and 3. This confirms that the floor-to-column pounding leads to the amplification of the shear forces
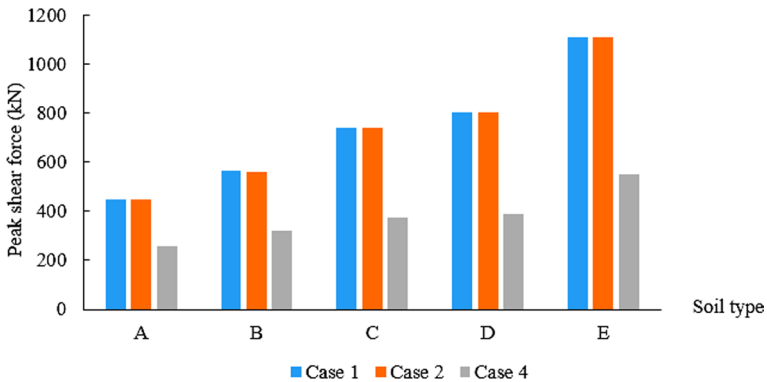
Table 3 Peak shear forces (kN) experienced in column C4 for the 4-7 pounding scenario and the ratio of the peak shear force for the 4-7 pounding scenario to that of the no pounding case

| Soil type	Peak shear force (kN)			Ratio of peak shear force of Case 1 to Case 4	Ratio of peak shear force of Case 2 to Case 4
	Case 1	Case 2	Case 4		
A	449.7	449.1	256.1	1.8	1.8
B	562.1	561.4	320.1	1.8	1.8
C	739.9	739.9	376.6	2.0	2.0
D	801.1	800.6	388.2	2.1	2.1
E	1107.7	1108.4	550.1	2.0	2.0

Table 4 Peak shear forces (kN) experienced in column C4 for the 4-6 pounding scenario and the ratio of the peak shear force for the 4-7 pounding scenario to that of the no pounding case

Soil type	Peak shear force (kN)			Ratio of peak shear force of Case 1 to Case 4	Ratio of peak shear force of Case 2 to Case 4
	Case 1	Case 2	Case 4		
A	401.1	401.0	176.9	2.3	2.3
B	501.3	501.3	221.1	2.3	2.3
C	630.6	630.7	275.4	2.3	2.3
D	741.6	741.7	322.9	2.3	2.3
E	915.9	915.7	402.4	2.3	2.3

Fig. 5 Peak shear forces (kN) experienced in column C4 for the 4-7 pounding scenario
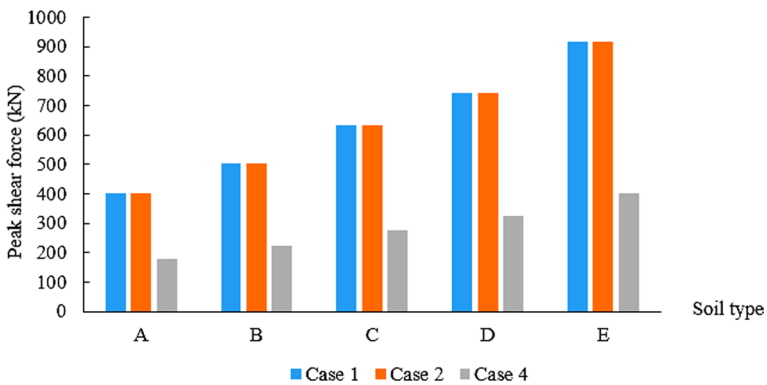
Fig. 6 Peak shear forces (kN) experienced in column C4 for the 4-6 pounding scenario

in the impacted columns compared to the no pounding scenario in all cases. Moreover, Tables 5 and 6 present the comparison between the shear strength of the impacted column (C4) and the peak shear forces developed due to the floor-to-column pounding. Also, the ratio between the peak shear forces of the impacted column (C4) in cases 1, 2 and 4 for the 4-7 and 4-6 pounding scenarios and the shear strength has been calculated also in Tables 5

Table 5 Peak shear forces (kN) experienced in column C4 for the 4-7 pounding scenario and the ratio of the peak shear force to the shear strength

Soil type	Shear strength (kN)	Peak shear force (kN) Case 1	Ratio	Peak shear force (kN) Case 2	Ratio	Peak shear force (kN) Case 4	Ratio
A	138.0	449.7	3.3	449.1	3.3	256.1	1.9
B	138.0	562.1	4.1	561.4	4.1	320.1	2.3
C	138.0	739.9	5.4	739.9	5.4	376.6	2.7
D	138.0	801.1	5.8	800.6	5.8	388.2	2.8
E	138.0	1107.7	8.0	1108.4	8.0	550.1	4.0

Table 6 Peak shear forces (kN) experienced in column C4 for the 4-6 pounding scenario and the ratio of the peak shear force to the shear strength

Soil type	Shear strength (kN)	Peak shear force (kN) Case 1	Ratio	Peak shear force (kN) Case 2	Ratio	Peak shear force (kN) Case 4	Ratio
A	138.0	401.1	2.9	401.0	2.9	176.9	1.3
B	138.0	501.3	3.6	501.3	3.6	221.1	1.6
C	138.0	630.6	4.6	630.7	4.6	275.4	2.0
D	138.0	741.6	5.4	741.7	5.4	322.9	2.3
E	138.0	915.9	6.6	915.7	6.6	402.4	2.9

and 6, respectively. It can be seen this ratio ranges between 1 and 8. This means that the impacted column experiences shear forces higher than the shear strength in all cases which, in fact, leads to brittle failure. This explains the brittle failure experienced by the columns that experienced floor-to-column pounding in previous earthquakes. Therefore, floor-to-column pounding has a significant effect on the shear demands of the impacted column. The local response of the impacted column can be considered as the most important issue in the floor-to-column pounding.

4 Floor-to-column pounding of buildings founded on different soil types

In this section, the effects of pounding on the impacted column of buildings founded on different soil types are analysed. Tables 7, 8, 9, 10 and 11 present the peak shear forces of the columns C1, C2, C3, C5 and C6, respectively, in the cases 1, 2 and 3 for the 4-7 pounding scenario. The graphical representation of these results is also shown in Figs. 7, 8, 9, 10 and 11. In addition, Tables 12, 13, 14, 15 and 16 present the peak shear forces of the columns C1, C2, C3, C5 and C6, respectively, in the cases 1, 2 and 3 for the 4-6 pounding scenario. The graphical representation of these results is also shown in Figs. 12, 13, 14, 15 and 16. As it can be seen, higher peak shear forces were experienced in the impacted column of the buildings founded on soil types E, then soil type D, then soil type C, then soil type B and finally soil type A. For instance, column

Table 7 Peak shear forces (kN) experienced in column C1 for the 4-7 pounding scenario and the ratio of the peak shear force to the shear strength

Soil type	Shear strength (kN)	Peak Shear force (kN) Case 1	Ratio	Peak shear force (kN) Case 2	Ratio	Peak shear force (kN) Case 3	Ratio
A	66.1	211.7	3.2	212.1	3.2	212.4	3.2
B	66.1	264.6	4.0	265.1	4.0	265.5	4.0
C	66.1	306.2	4.6	306.3	4.6	306.2	4.6
D	66.1	314.3	4.8	313.8	4.7	313.5	4.7
E	66.1	446.4	6.8	446.8	6.8	446.9	6.8

Table 8 Peak shear forces (kN) experienced in column C2 for the 4-7 pounding scenario and the ratio of the peak shear force to the shear strength

Soil type	Shear strength (kN)	Peak shear force (kN) Case 1	Ratio	Peak shear force (kN) Case 2	Ratio	Peak shear force (kN) Case 3	Ratio
A	138.0	260.7	1.9	261.1	1.9	261.5	1.9
B	138.0	325.9	2.4	326.4	2.4	326.9	2.4
C	138.0	378.4	2.7	378.5	2.7	378.4	2.7
D	138.0	388.9	2.8	388.2	2.8	387.9	2.8
E	138.0	552.0	4.0	552.4	4.0	552.6	4.0

Table 9 Peak shear forces (kN) experienced in column C3 for the 4-7 pounding scenario and the ratio of the peak shear force to the shear strength

Soil type	Shear strength (kN)	Peak shear force (kN) Case 1	Ratio	Peak shear force (kN) Case 2	Ratio	Peak shear force (kN) Case 3	Ratio
A	138.0	260.6	1.9	260.9	1.9	261.2	1.9
B	138.0	325.7	2.4	326.1	2.4	326.5	2.4
C	138.0	377.6	2.7	377.7	2.7	377.6	2.7
D	138.0	387.9	2.8	387.3	2.8	387.0	2.8
E	138.0	550.8	4.0	551.2	4.0	551.4	4.0

C1 in case 1 for the 4-7 pounding scenario has experienced peak shear forces of 446.4 kN for soil type E, 314.3 kN for soil type D, 306.2 kN for soil type C, 264.6 kN for soil type B and 211.7 kN for soil type A. Furthermore, Tables 7, 8, 9, 10, 11, 12, 13, 14, 15 and 16 also present the comparison between the shear strength of the impacted columns (C1, C2, C3, C5 and C6) and the peak shear forces developed due to the floor-to-column pounding. Also, the ratio between the peak shear forces of the impacted columns (C1, C2, C3, C5 and C6) in cases 1, 2 and 3 for the 4-7 and 4-6 pounding scenarios and the shear strength have been calculated also in Tables 7, 8, 9, 10, 11, 12, 13, 14, 15 and 16. It can be seen this ratio ranges between 1 and 7. This means that the impacted columns
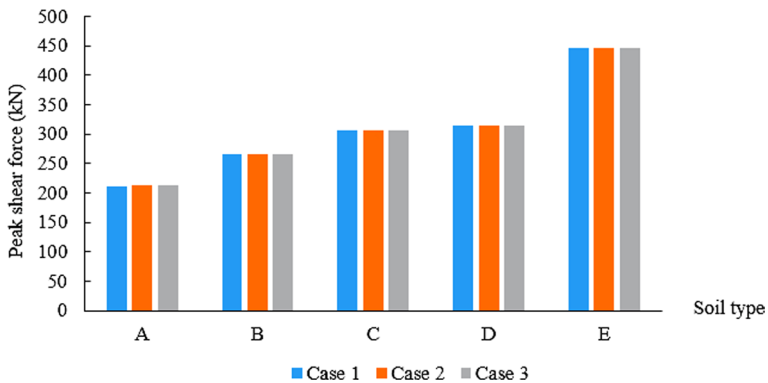
Table 10 Peak shear forces (kN) experienced in column C5 for the 4-7 pounding scenario and the ratio of the peak shear force to the shear strength

Soil type	Shear strength (kN)	Peak shear force (kN) Case 1	Ratio	Peak shear force (kN) Case 2	Ratio	Peak shear force (kN) Case 3	Ratio
A	138.0	261.5	1.9	261.6	1.9	261.8	1.9
B	138.0	326.9	2.4	327.0	2.4	327.3	2.4
C	138.0	378.4	2.7	378.4	2.7	378.4	2.7
D	138.0	388.6	2.8	388.0	2.8	387.7	2.8
E	138.0	551.9	4.0	552.5	4.0	552.6	4.0

Table 11 Peak shear forces (kN) experienced in column C6 for the 4-7 pounding scenario and the ratio of the peak shear force to the shear strength

Soil type	Shear strength (kN)	Peak shear force (kN) Case 1	Ratio	Peak shear force (kN) Case 2	Ratio	Peak shear force (kN) Case 3	Ratio
A	66.1	212.8	3.2	212.7	3.2	212.9	3.2
B	66.1	266.0	4.0	265.9	4.0	224.5	3.4
C	66.1	306.3	4.6	306.4	4.6	306.3	4.6
D	66.1	314.1	4.8	313.6	4.7	313.3	4.7
E	66.1	446.4	6.8	446.9	6.8	447.0	6.8

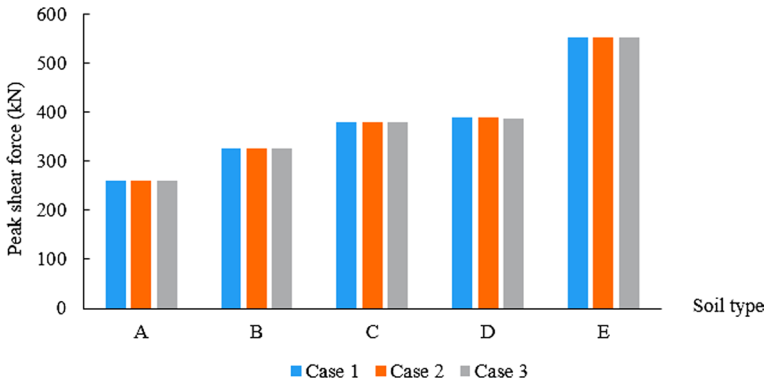**Fig. 7** Peak shear forces (kN) experienced in column C1 for the 4-7 pounding scenario

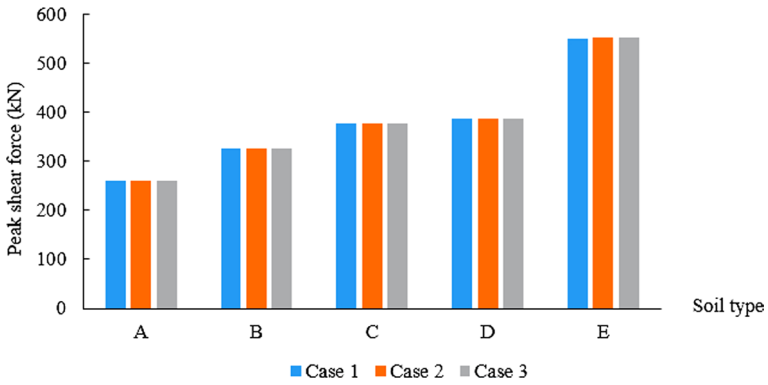**Fig. 8** Peak shear forces (kN) experienced in column C2 for the 4-7 pounding scenario

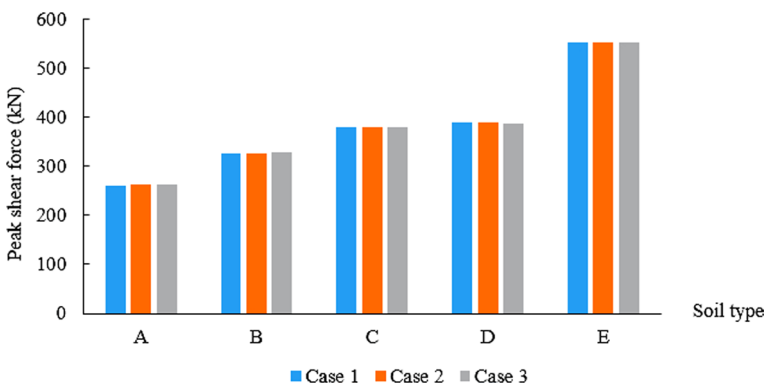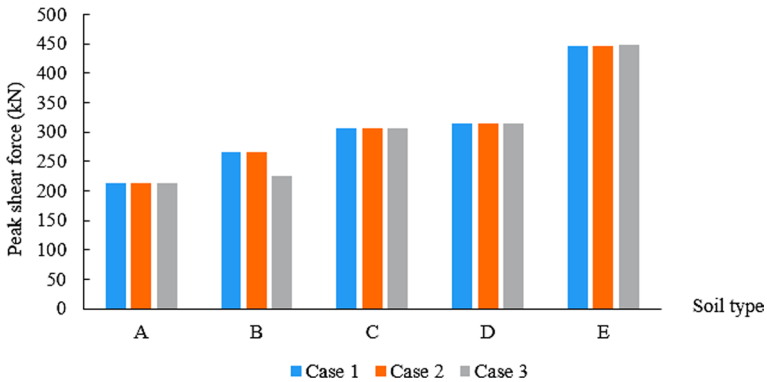**Fig. 9** Peak shear forces (kN) experienced in column C3 for the 4-7 pounding scenario

Fig. 10 Peak shear forces (kN) experienced in column C5 for the 4-7 pounding scenario

Fig. 11 Peak shear forces (kN) experienced in column C6 for the 4-7 pounding scenario

Table 12 Peak shear forces (kN) experienced in column C1 for the 4-6 pounding scenario and the ratio of the peak shear force to the shear strength

Soil type	Shear strength (kN)	Peak shear force (kN) Case 1	Ratio	Peak shear force (kN) Case 2	Ratio	Peak shear force (kN) Case 3	Ratio
A	66.1	145.0	2.2	144.9	2.2	145.2	2.2
B	66.1	181.3	2.7	181.2	2.7	181.4	2.7
C	66.1	243.4	3.7	243.3	3.7	247.2	3.7
D	66.1	264.4	4.0	264.3	4.0	264.5	4.0
E	66.1	325.7	4.9	326.3	4.9	324.7	4.9

Table 13 Peak shear forces (kN) experienced in column C2 for the 4-6 pounding scenario and the ratio of the peak shear force to the shear strength

Soil type	Shear strength (kN)	Peak shear force (kN) Case 1	Ratio	Peak shear force (kN) Case 2	Ratio	Peak shear force (kN) Case 3	Ratio
A	138.0	177.7	1.3	177.7	1.3	177.9	1.3
B	138.0	222.2	1.6	222.1	1.6	222.4	1.6
C	138.0	296.5	2.1	296.3	2.1	300.9	2.2
D	138.0	324.2	2.3	324.1	2.3	324.3	2.4
E	138.0	399.4	2.9	400.1	2.9	398.2	2.9

Table 14 Peak shear forces (kN) experienced in column C3 for the 4-6 pounding scenario and the ratio of the peak shear force to the shear strength

Soil type	Shear strength (kN)	Peak shear force (kN) Case 1	Ratio	Peak shear force (kN) Case 2	Ratio	Peak shear force (kN) Case 3	Ratio
A	138.0	177.4	1.3	177.3	1.3	177.6	1.3
B	138.0	221.8	1.6	221.6	1.6	221.9	1.6
C	138.0	296.2	2.1	296.0	2.1	300.6	2.2
D	138.0	323.5	2.3	323.4	2.3	323.7	2.3
E	138.0	398.6	2.9	399.2	2.9	397.4	2.9

Table 15 Peak shear forces (kN) experienced in column C5 for the 4-6 pounding scenario and the ratio of the peak shear force to the shear strength

Soil type	Shear strength (kN)	Peak shear force (kN) Case 1	Ratio	Peak shear force (kN) Case 2	Ratio	Peak shear force (kN) Case 3	Ratio
A	138.0	177.8	1.3	177.7	1.3	177.9	1.3
B	138.0	222.2	1.6	222.1	1.6	222.4	1.6
C	138.0	296.7	2.1	296.3	2.1	300.9	2.2
D	138.0	324.2	2.3	324.0	2.3	324.3	2.3
E	138.0	399.4	2.9	400.0	2.9	398.2	2.9

Table 16 Peak shear forces (kN) experienced in column C6 for the 4-6 pounding scenario and the ratio of the peak shear force to the shear strength

Soil type	Shear strength (kN)	Peak shear force (kN) Case 1	Ratio	Peak shear force (kN) Case 2	Ratio	Peak shear force (kN) Case 3	Ratio
A	66.1	145.1	2.2	145.0	2.2	145.2	2.2
B	66.1	181.3	2.7	181.2	2.7	181.5	2.7
C	66.1	243.8	3.7	243.4	3.7	247.1	3.7
D	66.1	264.5	4.0	264.3	4.0	264.6	4.0
E	66.1	325.8	4.9	326.3	4.9	324.8	4.9

experience shear forces higher than the shear strength in all cases which leads to brittle failure. This confirms the conclusions concluded in Sect. 3.

5 Conclusions

The effects of the soil type on buildings experiencing floor-to-column pounding during earthquakes were investigated in this study. Five buildings with 4-storeys, 6-storeys, and 7-storeys were considered. Three types of the 4-storey building with different total heights
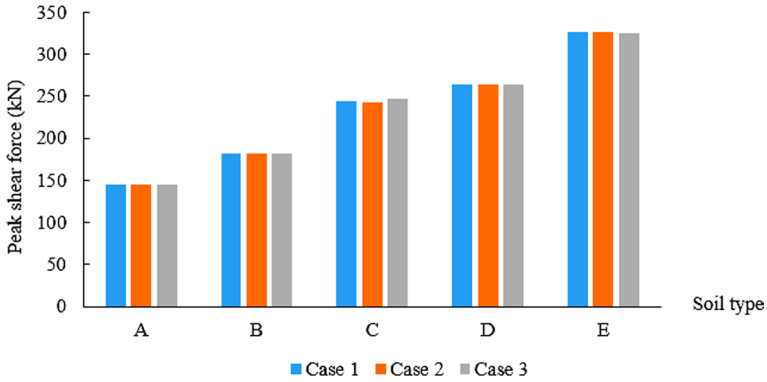
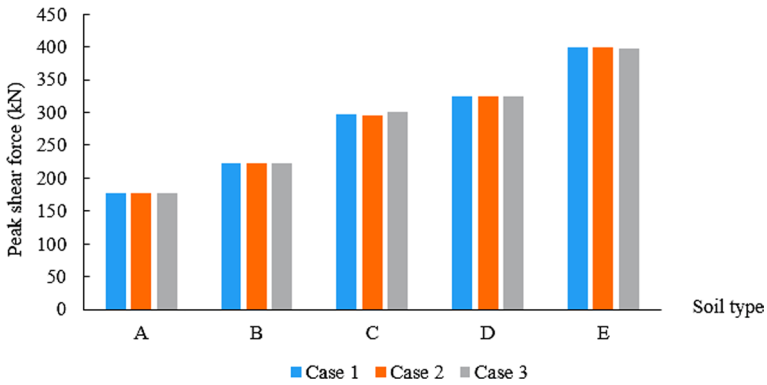**Fig. 12** Peak shear forces (kN) experienced in column C1 for the 4-6 pounding scenario

Fig. 13 Peak shear forces (kN) experienced in column C2 for the 4-6 pounding scenario
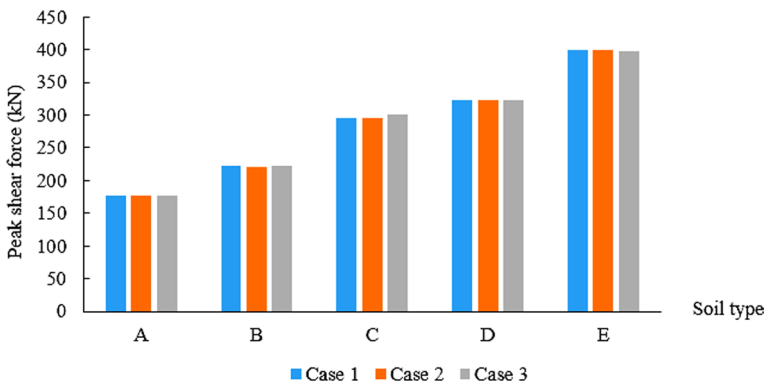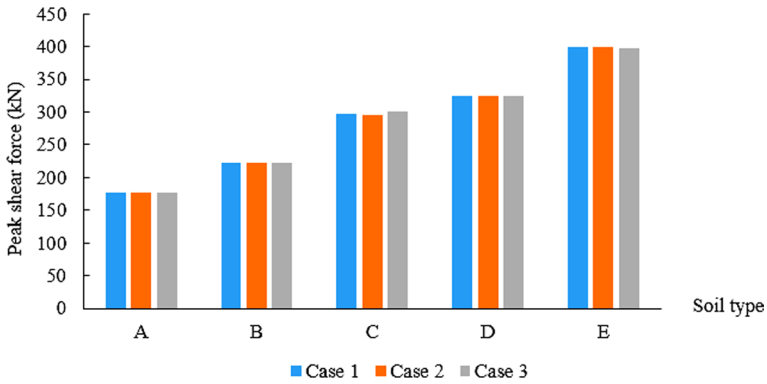

Fig. 14 Peak shear forces (kN) experienced in column C3 for the 4-6 pounding scenario

were taken into account which leads to floor-to-column pounding at 1/3, 1/2 and 2/3 of the height of the impacted column. Two pounding scenarios were considered, i.e. pounding between the 4-storey and 6-storey buildings and pounding between the 4-storey and

Fig. 15 Peak shear forces (kN) experienced in column C5 for the 4-6 pounding scenario
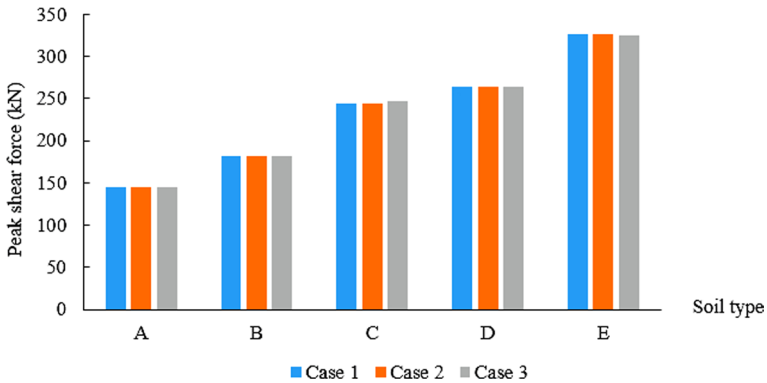
Fig. 16 Peak shear forces (kN) experienced in column C6 for the 4-6 pounding scenario

7-storey buildings. Firstly, the shear demands of the columns at the contact area were studied and compared with the no pounding case to investigate the effect of the floor-to-column pounding. Then, the shear demands of the columns at the contact area were studied for buildings founded on different soil types to investigate the effect of the soil type on the structural response.

The main conclusions of this study are:

- The shear demands of the impacted column significantly increase due to collisions in all analysed cases. The shear forces may be amplified even 2–3 times, compared to the no pounding case.
- The peak shear forces of the impacted columns due to floor-to-column pounding exceeds the shear strength in all cases. The ratio of the peak shear forces to that of the shear strength ranged between 1 and 8. In fact, this leads to the brittle failure of the impacted columns.
- The impacted column experiences higher shear demands for buildings founded on the soft clay soil, then for buildings founded on the stiff soil, then for buildings founded on very dense soil and soft rock, and finally for buildings founded on the rock and hard rock.

Declarations

Conflict of interests The authors declare that they have no conflict of interest.

References

Anagnostopoulos SA (1988) Pounding of buildings in series during earthquakes. Earthq Eng Struct Dyn 16:443–456

Anagnostopoulos S (1996) Building pounding re-examined: how serious a problem is it. In: Eleventh world conference on earthquake engineering. Pergamon, UK, p 2108

Behnamfar F, Banizadeh M (2016) Effects of soil–structure interaction on distribution of seismic vulnerability in RC structures. Soil Dyn Earthq Eng 80:73–86

Cole G, Dhakal R, Carr A, Bull D (2010a) Building pounding state of the art: identifying structures vulnerable to pounding damage. In: 2010a New Zealand Society of Earthquake Engineering (NZSEE) conference, New Zealand

Cole G, Dhakal R, Carr A, Bull D (2010b) Interbuilding pounding damage observed in the Darfield Earthquake. Bull N Z Soc Earthq Eng 43:382–386

Cole G, Dhakal R, Carr A, Bull D (2011) Case studies of observed pounding damage during the 2010c Darfield earthquake. In: 9th Pacific conference on earthquake engineering building an earthquake-resilient society, Auckland, New Zealand, pp 14–16

Cole G, Dhakal R, Chouw N (2012a) Building pounding damage observed in the 2011 Christchurch earthquake. In: 15th world conference on earthquake engineering

Cole GL, Dhakal RP, Turner FM (2012b) Building pounding damage observed in the 2011 Christchurch earthquake. Earthq Eng Struct Dyn 41:893–913

Computers and Structures I, Berkeley, California. CSI analysis reference manual For SAP 2000, ETABS, SAFE and CSI Bridge

Computers and Structures I, Berkeley, California. ETABS

Doğan M, Günaydin A (2009) Pounding of adjacent RC buildings during seismic loads. J Eng Archit Fac Eskişehir Osmangazi Univ 22:129–145

Efraimiadou S, Hatzigeorgiou GD, Beskos DE (2013) Structural pounding between adjacent buildings subjected to strong ground motions. Part I: the effect of different structures arrangement. Earthq Eng Struct Dyn 42:1509–1528

Elwardany H, Seleemah A, Jankowski R (2017) Seismic pounding behavior of multi-story buildings in series considering the effect of infill panels. Eng Struct 144:139–150

Elwardany H, Seleemah A, Jankowski R, El-Khoriby S (2019) Influence of soil-structure interaction on seismic pounding between steel frame buildings considering the effect of infill panels. Bull Earthq Eng 17:6165–6202

Farghaly AA (2017) Seismic analysis of adjacent buildings subjected to double pounding considering soil–structure interaction. Int J Adv Struct Eng 9:51–62

Fatahi B, Van Nguyen Q, Xu R, Sun W-J (2018) Three-dimensional response of neighboring buildings sitting on pile foundations to seismic pounding. Int J Geomech 18:04018007

Favvata MJ (2017) Minimum required separation gap for adjacent RC frames with potential inter-story seismic pounding. Eng Struct 152:643–659

Favvata MJ, Karayannis CG, Liolios AA (2009) Influence of exterior joint effect on the inter-story pounding interaction of structures. Struct Eng Mech 33:113–136

Ghandil M, Aldaikh H (2017) Damage-based seismic planar pounding analysis of adjacent symmetric buildings considering inelastic structure–soil–structure interaction. Earthq Eng Struct Dyn 46:1141–1159

Gong L, Hao H (2005) Analysis of coupled lateral-torsional-pounding responses of one-storey asymmetric adjacent structures subjected to bi-directional ground motions part I: uniform ground motion input. Adv Struct Eng 8:463–479

Ibrahimbegovic A, Wilson EL (1989) Simple numerical algorithms for the mode superposition analysis of linear structural systems with non-proportional damping. Comput Struct 33:523–531

Inel M, Cayci BT, Kamal M, Altinel O (2014) Structural pounding of mid-rise RC buildings during earthquakes. In: 2nd European conference on earthquake engineering and seismology

Jameel M, Islam A, Hussain RR, Hasan SD, Khaleel M (2013) Non-linear FEM analysis of seismic induced pounding between neighbouring multi-storey structures. Latin Am J Solids Struct 10:921–939

Jankowski R (2005) Impact force spectrum for damage assessment of earthquake-induced structural pounding. Key Eng Mater 293–294:711–718

Jankowski R (2006) Pounding force response spectrum under earthquake excitation. Eng Struct 28:1149–1161

Jankowski R (2007) Assessment of damage due to earthquake-induced pounding between the main building and the stairway tower. Key Eng Mater 347:339–344

Jankowski R (2008) Earthquake-induced pounding between equal height buildings with substantially different dynamic properties. Eng Struct 30:2818–2829

Jankowski R, Seleemah A, El-Khoriby S, Elwardany H (2015) Experimental study on pounding between structures during damaging earthquakes. Key Eng Mater 627:249–252

Kamgar R, Tavakoli R, Rahgozar P, Jankowski R (2021) Application of discrete wavelet transform in seismic nonlinear analysis of soil-structure interaction problems. Earthq Spectra 37:1980–2012

Karapetrou S, Fotopoulou S, Pitilakis K (2015) Seismic vulnerability assessment of high-rise non-ductile RC buildings considering soil–structure interaction effects. Soil Dyn Earthq Eng 73:42–57

Karayannis CG, Favvata MJ (2005a) Earthquake-induced interaction between adjacent reinforced concrete structures with non-equal heights. Earthq Eng Struct Dyn 34:1–20

Karayannis CG, Favvata MJ (2005b) Inter-story pounding between multistory reinforced concrete structures. Struct Eng Mech 20:505–526

Karayannis CG, Naoum MC (2017) Inter-story pounding and torsional effect due to interaction between adjacent multistory RC buildings. In: 6th ECCOMAS thematic conference on computational methods in structural dynamics and earthquake engineering, Greece

Karayannis CG, Naoum MC (2018) Torsional behavior of multistory RC frame structures due to asymmetric seismic interaction. Eng Struct 163:93–111

Karayannis CG, Kakaletsis D, Favvata M (2005) Behavior of bare and masonry infilled R/C frames under cyclic loading: experiments and analysis. WIT Trans Built Environ 81

Karayannis CG, Favvata MJ, Kakaletsis D (2011) Seismic behaviour of infilled and pilotis RC frame structures with beam–column joint degradation effect. Eng Struct 33:2821–2831

Kasai K, Maison BF (1997) Building pounding damage during the 1989 Loma Prieta earthquake. Eng Struct 19:195–207

Kazemi F, Miari M, Jankowski R (2021) Investigating the effects of structural pounding on the seismic performance of adjacent RC and steel MRFs. Bull Earthq Eng 19:317–343

Kontoni D-PN, Farghaly AA (2018) Seismic response of adjacent unequal buildings subjected to double pounding considering soil-structure interaction. Computation 6:10

Korzec A, Jankowski R (2021) Extended Newmark method to assess stability of slope under bidirectional seismic loading. Soil Dyn Earthq Eng 143:106600

Li P, Liu S, Lu Z (2017) Studies on pounding response considering structure-soil-structure interaction under seismic loads. Sustainability 9:2219

Madani B, Behnamfar F, Riahi HT (2015) Dynamic response of structures subjected to pounding and structure–soil–structure interaction. Soil Dyn Earthq Eng 78:46–60

Mahmoud S, Jankowski R (2009) Elastic and inelastic multi-storey buildings under earthquake excitation with the effect of pounding. J Appl Sci 9:3250–3262

Mahmoud S, Chen X, Jankowski R (2008) Structural pounding models with Hertz spring and nonlinear damper. J Appl Sci 8:1850–1858

Mahmoud S, Abd-Elhamed A, Jankowski R (2013) Earthquake-induced pounding between equal height multi-storey buildings considering soil-structure interaction. Bull Earthq Eng 11:1021–1048

Maison BF, Kasai K (1992) Dynamics of pounding when two buildings collide. Earthq Eng Struct Dyn 21:771–786

Mavronicola EA, Polycarpou PC, Komodromos P (2020) Effect of ground motion directionality on the seismic response of base isolated buildings pounding against adjacent structures. Eng Struct 207:110202

Miari M, Jankowski R (2021) Pounding between high-rise buildings founded on different soil types. In: 17th world conference on earthquake engineering, Sendai, Japan

Miari M, Jankowski R (2022a) Incremental dynamic analysis and fragility assessment of buildings with different structural arrangements experiencing earthquake-induced structural pounding. In: International conference on computational science, London, United Kingdom

Miari M, Jankowski R (2022b) Analysis of pounding between adjacent buildings founded on different soil types. Soil Dyn Earthq Eng 154:107156

Miari M, Jankowski R (2022c) Incremental dynamic analysis and fragility assessment of buildings founded on different soil types experiencing structural pounding during earthquakes. Eng Struct 252:113118

Miari M, Jankowski R (2022d) Seismic gap between buildings founded on different soil types experiencing pounding during earthquakes. Earthq Spectra. https://doi.org/10.1177/87552930221082968

Miari M, Choong KK, Jankowski R (2019) Seismic pounding between adjacent buildings: identification of parameters, soil interaction issues and mitigation measures. Soil Dyn Earthq Eng 121:135–150

Miari M, Choong KK, Jankowski R (2021) Seismic pounding between bridge segments: a state-of-the-art review. Arch Comput Methods Eng 28:495–504

Minimum Design Loads for Buildings and Other Structures (ASCE/SEI 7-10). American Society of Civil Engineers

Mouzakis HP, Papadrakakis M (2004) Three dimensional nonlinear building pounding with friction during earthquakes. J Earthq Eng 8:107–132

Naserkhaki S, Aziz FNA, Pourmohammad H (2012) Earthquake induced pounding between adjacent buildings considering soil-structure interaction. Earthq Eng Eng Vib 11:343–358

Naserkhaki S, El Rich M, Abdul AF, Pourmohammad H (2013) Separation gap, a critical factor in earthquake induced pounding between adjacent buildings. Asian J Civ Eng (BHRC) 14:881–898

Naserkhaki S, El-Rich M, Aziz F, Pourmohammad H (2014) Pounding between adjacent buildings of varying height coupled through soil. Struct Eng Mech 52:573–593

Pacific Earthquake Engineering Research Centre (PEER NGA DATABASE). http://peer.berkeley.edu/nga

Raheem SEA (2006) Seismic pounding between adjacent building structures. Electron J Struct Eng 6:155

Raheem SEA (2014) Mitigation measures for earthquake induced pounding effects on seismic performance of adjacent buildings. Bull Earthq Eng 12:1705–1724

Rajaram C, Kumar RP (2012) Three dimensional modeling of pounding between adjacent buildings. In: Fourth international conference on structural stability and dynamics (ICSSD 2012), Malaviya National Institute of Technology, Jaipur & Texas A&M University, USA, pp 4–6

Requena-Garcia-Cruz M, Bento R, Durand-Neyra P, Morales-Esteban A (2022) Analysis of the soil structure-interaction effects on the seismic vulnerability of mid-rise RC buildings in Lisbon. Structures 38:599–617

Rezaei H, Moayyedi SA, Jankowski R (2020) Probabilistic seismic assessment of RC box-girder highway bridges with unequal-height piers subjected to earthquake-induced pounding. Bull Earthq Eng 18:1547–1578

Rojas FR, Anderson JC (2012) Pounding of an 18-story building during recorded earthquakes. J Struct Eng 138:1530–1544

Rosenblueth E, Meli R (1986) The 1986 Mexico earthquake. Concr Int 8:23–34

Shakya K, Wijeyewickrema AC, Ohmachi T (2008) Mid-column seismic pounding of reinforced concrete buildings in a row considering effects of soil. In: 14th world conference on earthquake engineering, pp 12–17

Shakya K, Wijeyewickrema AC (2009) Mid-column pounding of multi-story reinforced concrete buildings considering soil effects. Adv Struct Eng 12:71–85

Sołtysik B, Jankowski R (2013) Non-linear strain rate analysis of earthquake-induced pounding between steel buildings. Int J Earth Sci Eng 6:429–433

Sołtysik B, Jankowski R (2015) Building damage due to structural pounding during earthquakes. J Phys Conf Ser 628:012040

Stewart JP, Fenves GL, Seed RB (1999) Seismic soil-structure interaction in buildings. I: analytical methods. J Geotech Geoenviron Eng 125:26–37